

**Enhancement of the magnetic refrigerant capacity in partially amorphous Fe<sub>70</sub>Zr<sub>30</sub> powders obtained by mechanical alloying**

J. S. Blázquez\*, V. Franco, A. Conde

Departamento de Física de la Materia Condensada, Universidad de Sevilla, P. O. Box 1065, 41080, Sevilla, Spain.

**Abstract**

After mechanical alloying Fe<sub>70</sub>Zr<sub>30</sub> composition from pure starting powders, an amorphous phase with Curie temperature T<sub>C</sub>=244 K and an intermetallic compound (that should be non-stoichiometric Zr rich fcc Fe<sub>2</sub>Zr phase) with T<sub>C</sub>=355 K are formed. Residual α-Fe crystallites are also found. The multiphase character of this system yields a non-monotonic dependence of the magnetocaloric effect (characterized by the refrigerant capacity, RC) on the fraction of phases. Among the samples studied in this work, RC is enhanced for samples with the highest fraction of intermetallic compound, although the maximum magnetic entropy change monotonically decreases with the increase of the fraction of this phase. This behaviour agrees with the predicted one for biphasic systems.

**Keywords:** A. nanostructured intermetallics; A. magnetic intermetallics; B. magnetic properties; C. mechanical alloying and milling.

\*Corresponding author: J. S. Blázquez

Departamento de Física de la Materia Condensada. Universidad de Sevilla.

Apartado 1065, 41080 Sevilla (Spain).

Phone: (34) 95 455 60 29/ Fax: (34) 95 461 20 97

E-mail: [jsebas@us.es](mailto:jsebas@us.es)

## 1. Introduction

Magnetocaloric effect (MCE) at room temperature is a subject of intense study in recent years as magnetic refrigeration shows several promising advantages over conventional refrigerant techniques based on gas expansion-compression cycles (e.g. noise free and environmental friendly as it does not use ozone depleting gases) [1]. Room temperature refrigeration requires the presence of a magnetic transition at which a sharp change of magnetization,  $M$ , with temperature,  $T$ , occurs, which maximizes the magnetic entropy change,  $\Delta S_M$ , ascribed to it. The latter magnitude can be calculated from  $M(H,T)$  curves (being  $H$  the maximum applied field) using Maxwell relation:

$$\Delta S_M(T, H) = \int_0^H \left. \frac{\partial M}{\partial T} \right|_H dT$$

In the case of room temperature applications, there should be a certain temperature range in which the magnetic entropy change of the material must be relatively high. A measure of the relationship between peak height and peak width is given by the refrigerant capacity,  $RC$ , which is an useful magnitude to compare different materials and is related to the energy per unit mass ascribed to the adiabatic magnetization process. Three are the main ways to define  $RC$  for a given maximum applied field:

- $RC_{AREA}$  is the area below  $\Delta S_M(T)$  curve between the temperatures  $T_{Cold}$  and  $T_{Hot}$  ( $T_{Hot} > T_{Cold}$ ) at which  $\Delta S_M(T_{Cold}) = \Delta S_M(T_{Hot}) = \Delta S_M(T_{Peak})/2$ , where  $T_{Peak}$  is the temperature at which  $\Delta S_M$  is maximum;
- $RC_{FWHM} = (T_{Hot} - T_{Cold}) \cdot \Delta S_M(T_{Peak})$ ;
- $RC_{WP}$ , which is defined after Wood and Potter [2] as the maximum rectangular area which can be inscribed into  $\Delta S_M$  curve. In this definition, the cold and hot temperatures are different to the previously defined ones.

Two lines of study of MCE materials can be established: one based on materials which suffer a first order magnetic/magnetostructural phase transition and the other based on materials suffering a second order magnetic transition. The former line yields materials with the highest  $\Delta S_M(T_{\text{Peak}})$  values and the term giant magnetocaloric effect (GMCE) was coined to describe this behaviour. However, thermal and magnetic hysteresis is a drawback inherent to these materials. The second line tries to look for enhancement of MCE mainly by broadening the  $\Delta S_M(T)$  curves, i.e enhancing RC, although  $\Delta S_M(T_{\text{Peak}})$  is well below the values exhibited by GMCE materials. Elemental Gd, with a Curie temperature  $T_C=295$  K,  $\Delta S_M(T_{\text{Peak}})=6$  J kg<sup>-1</sup> K<sup>-1</sup> and  $RC_{\text{FWHM}}=240$  J kg<sup>-1</sup> for  $H=2$  T, belongs to this line and is the main material used in the development of prototypes for magnetic refrigeration [1].

Recently, it has been proposed that the use of multiphase systems is a suitable choice to obtain RC enhancement [3,4,5,6]. Particularly, when the difference between the Curie temperature of the constituent phases is around 100 K and the fraction of the phase with the highest Curie is above 50 %, an important enhancement can be obtained [3] as confirmed by experiments on composites of two Fe based amorphous alloys [4]. These Fe based, rare earth free, systems have the additional advantage of the low cost of the material in comparison with Gd or other rare earth based materials.

It would be very convenient if the different phases constituting the multiphase system were produced in a single step in order to minimize production cost and to achieve a more intimate contact between the phases, which would allow to optimize the behaviour through tailoring interactions between phases and the distribution exchange inside them [7]. This is the case of nanocrystalline systems, where ~5-10 nm nanocrystals are embedded in a residual amorphous matrix. However, although the amorphous phase can exhibit Curie temperatures close to room temperature for some

compositions [8], the bcc-Fe type nanocrystals generally formed have a much larger Curie temperature,  $\sim 1043$  K for pure Fe, and yields a progressive impoverishment of the MCE signal, either if they appear after controlled crystallization of a precursor amorphous [9,10] or as a remaining phase after ball milling [11,12].

Recent studies [13] performed at room temperature on mechanically alloyed  $\text{Fe}_{70}\text{Zr}_{30}$  composition (starting from pure powders) showed a weak magnetic phase at room temperature embedded in a paramagnetic amorphous phase. The aim of the present work is to show that the presence of this magnetic phase with a Curie temperature  $\sim 100$  K above that of the amorphous matrix is the responsible for a clear enhancement of RC.

## 2. Experimental

Partially amorphous  $\text{Fe}_{70}\text{Zr}_{30}$  powder samples were produced by ball milling using two equivalent milling processes (details can be found elsewhere [13]). Each milling step corresponds to 4 (8) additional hours of milling at 360 (286) rpm. These two milling processes are expected to be equivalent according to the cubic law of the power released to the powder during milling [14], as the cube of the ratio between these two frequencies is  $(360/286)^3=2$ . After the first milling step and for both cases (8 h at 286 and 4 h at 360 rpm), no powder could be recover as it was completely pasted on the milling media forming a shiny surface. The maximum accumulated milling times were 24 and 48 h at 360 and 286 rpm, respectively (6 milling steps).

XRD patterns of as-milled powders (some examples are shown in figure 1) show typical amorphous halos. For samples milled after the second milling step, weak evidences of intermetallic peaks could be pointed. However, as the size of this intermetallic must be very small (typically  $\sim 5$  nm [15]) and the main diffraction peaks

strongly overlap with the halo, a quantitative analysis was prevented. The angular positions of these weak peaks are in agreement with those of fcc Fe<sub>2</sub>Zr phase, which is the phase developed after heat treatment [13], as also shown in Fig. 1.

As differential scanning calorimetry (DSC) results show [13], the powder is thermally stable up to 400 K. At this temperature, desorption of gases might occur in agreement with a decrease of the weight of the samples. It is worth noticing that deviations at ~400 K from DSC baseline are generally observed for Fe based ball milled powders. Thus Mössbauer (MS) experiments were performed from room temperature up to 400 K. MS spectra were recorded in a transmission geometry using a <sup>57</sup>Co(Rh) source. The values of the hyperfine parameters were obtained by fitting with NORMOS program [16]. The isomer shift, IS, was quoted relative to the Mössbauer spectrum of an  $\alpha$ -Fe foil at room temperature.

The field dependence of magnetization, M(H), was measured using a Lakeshore 7407 Vibrating Sample Magnetometer (VSM) using a maximum applied field  $\mu_0H=1.5$  T, with field steps of 0.025 T, for constant temperatures in the range of  $90 \leq T \leq 400$  K with increments of 10 K. The magnetic entropy change due to the application of a maximum magnetic field H has been calculated from the numerical derivative of the M(H,T) curves with respect to temperature and subsequent integration in field.

### **3. Results**

#### *3.1 MCE results*

Figure 2 shows  $\Delta S_M(T)$  curves for a maximum applied field  $\mu_0H=1.5$  T for the different studied samples. An increase of  $|\Delta S_M|$  at the peak is clearly observed as milling increases, i. e. as amorphous fraction increases. This behaviour is typically observed for

other partially amorphous alloys [11,12]. However, for those systems, the remaining crystallites have a Curie temperature well separated from that of the amorphous phase, which has been shown to deteriorate the MCE response in terms of the RC value. However, for the present alloy, RC does not decrease as  $|\Delta S_M|$  does but the highest values were observed for the samples with the lowest amorphous fraction of this study (obtained after the second milling step) as shown in figure 3. For these samples,  $\Delta S_M$  curve becomes very broad and the half value of  $\Delta S_M(T_{Peak})$  is not reached below 400 K. Therefore, the actual RC values for these samples must be even higher. Temperature increase beyond 400 K has been avoided in order to prevent sample evolution as commented before. Similar values  $<100$  J/kg at  $H=1.5$  T were found for other partially amorphous Fe-based alloys obtained by ball milling, [11,12] which are comparable or even superior to other alloy systems [17,18].

In order to measure the Curie temperature of the different phases, low field magnetization curves were analyzed. The  $M(T)$  curve at  $\mu_0 H=0.05$  T is shown in figure 4 for the sample milled at 286 rpm after the second milling step. The inset of Fig. 4 shows the thermal derivative of magnetization. The inflexion points detected are  $T_C^{Am}=244$  K, in agreement with the maximum of the  $\Delta S_M(T)$  curve and thus corresponding to the amorphous phase, and  $T_C^{Int}=355$  K, in agreement with the magnetic contribution with  $HF < 20$  T detected after room temperature Mössbauer experiments [13]. However, these peaks are not sharp but very broad, which can be ascribed to a distribution of transition temperatures in both phases. This fact, typically found in amorphous systems [7], is enhanced by using ball milling as heterogeneities and impurities are inherent to the production technique [15]. In our case, this aspect contributes to broaden the MCE signal.

As commented above, XRD results indicate that this intermetallic compound could be fcc Fe<sub>2</sub>Zr phase. However, the stoichiometric 2:1 phase exhibits a much higher Curie temperature than 355 K. This fact should prevent the identification of the intermetallic formed during milling and responsible of RC enhancement as fcc Fe<sub>2</sub>Zr. However, it is worth mentioning the work of Kiss et al. [19] on Fe<sub>100-x</sub>Zr<sub>x</sub> ingots, where they described the compositional dependence of this intermetallic. Kiss et al. measured a strong decrease of the Curie temperature from 790 to 630 K as x increases from 29 to 33 %. If this linear trend is extrapolated, taking into account that supersaturated solutions are easily found as ball milling products [15], the T<sub>C</sub> of the intermetallic compound detected in the present work would match that of a fcc Fe<sub>2</sub>Zr phase with ~40 at. % of Zr. Similar result can be obtained using the data from Mattern et al. [20]. Thus it is plausible to identify the intermetallic compound formed during ball milling as a Zr rich Fe<sub>2</sub>Zr phase.

### 3.2 Mössbauer results

Some examples of experimental Mössbauer spectra along with their corresponding fitting curves are shown in figure 5. The presence of HF contributions different to that of  $\alpha$ -Fe type residual crystallites can be clearly observed as a hump close to the central absorption line for the powder after the second milling step. This hump is less appreciable in samples after the sixth milling step. As temperature increase, the hump becomes merged with the central line.

In general, three contributions have been used to fit the spectra: a sextet ascribed to residual bcc-Fe crystallites, a hyperfine field distribution (HFD) extended up to about 20 T and a quadrupole distribution (QD). The ascription of HFD to the phase with T<sub>C</sub>=355 K and QD to the amorphous matrix (with a T<sub>C</sub>=244 K and thus below the

thermal range explored here using Mössbauer spectrometry) is not straightforward. In fact, there is some ambiguity in fitting the different possible contributions to the central absorption line. Both low fields ( $HF \sim < 5$  T) of the hyperfine field distribution and quadrupolar distribution can contribute to this line. Therefore the average hyperfine field has been measured considering  $HF = 0$  T for all those contributions with hyperfine field below 5 T. This will assure the different fittings are comparable. As an example, the average HF values of the spectra (considering zero for QD and HFD contributions  $\leq 5$  T) are shown in Fig. 4 for the sample milled at 286 rpm after the second milling step. The straight lines correspond to linear fitting above and below  $T_C^{Int}$  (due to the small temperature range explored). In this representation,  $T_C^{Int}$  is clearly identified and in very good agreement with the results from VSM. In order to reduce the number of free parameters, the HF values of  $\alpha$ -Fe phase was fixed using the average results of fitting at room temperature, 32.3 T (lower than that of pure Fe due to presence of Zr atoms), and a linear decrease of 0.5 T as temperature increases from 300 to 400 K, following Ref. [21,22].

Figure 6 shows the average IS values and the fraction of Fe atoms contributing to HFD with  $HF > 5$  T as a function of the temperature of measurement. The former magnitude decreases as T increases as expected from second order Doppler shift effect [23]. The latter magnitude is a measurement of the magnetism ascribed to the intermetallic compound. The amount of this phase remains constant in the explored thermal range (there is no microstructural evolution during MS experiments) but the fraction plotted in figure 6 decreases as the Curie temperature of the intermetallic compound is approached and overcome. The average value of the quadrupolar splitting is almost constant and  $\sim 0.45$  mm/s.



#### 4. Discussion

Non-monotonic variations of RC with the fraction of phases in two phase systems have been predicted theoretically for non-interacting systems [3]. Enhancement of RC over the values of the single phase systems depends on fraction of phases, difference in Curie temperatures as well as maximum applied field. Figure 7 shows the observed experimental dependence of  $RC_{FWHM}$  in this study as a function of the fraction of Mössbauer contributions above 5 T (not including  $\alpha$ -Fe contribution),  $x_{HF>5T}$ . This fraction should only correspond to part of the fcc  $Fe_2Zr$  phase contribution as some low field contributions (Fe in  $Fe_2Zr$  phase with a high number of Zr as neighbours) have been merged in the central absorption line.

As the fraction of  $Fe_2Zr$  phase increases from very low values, a decrease of RC occurs. This is in agreement with the expected behaviour for low concentrations of the high  $T_C$  phase [3]. If we extrapolate the behaviour to a fraction zero, we can roughly estimate  $RC_{FWHM}$  of the amorphous phase below 75 J/kg. This value is below those achieved for  $x_{HF>5T} > \sim 30\%$  and thus an enhancement may have been achieved for this samples with respect to that expected for a completely amorphous sample.

However, the present system has a third phase:  $\alpha$ -Fe type impurities. The Curie temperature of this phase is well separated from those of the amorphous and the Zr-rich  $Fe_2Zr$  phases. Therefore, its contribution, for the thermal range explored and the field change used in this study, is expected to just decrease the MCE signal in a factor equal to its mass fraction. From Mössbauer experiments a  $\sim 5\%$  fraction is measured. This Mössbauer fraction is only over Fe atoms, thus 5 % of the Fe atoms in the alloy are in  $\alpha$ -Fe phase. Considering that Fe is only 70 at. % of the sample, 5 % of the Fe atoms in  $\alpha$ -Fe phase implies 3.5 at. % of this phase in the system. Moreover, considering the

atomic mass of Fe and Zr, the weight percentage of  $\alpha$ -Fe phase (and so the effect on MCE) can be estimated to be below 3 %.

As Fe is the only element in the studied samples having atomic magnetic moment, hyperfine field of the  $^{57}\text{Fe}$  atoms and saturation magnetization must show a linear behaviour. However, in order to check this linearity,  $\alpha$ -Fe phase must be taken into account, as the magnetic response per atom of this phase is the highest among the three phases in the system. To do so, technical saturation magnetization,  $M_S(0)$ , was calculated by extrapolating to zero field the linear behaviour of  $M(H)$  curves between 1 and 1.5 T. This can be observed in figure 8, where a global linearity between both magnitudes is fulfilled.

## 5. Conclusions

Refrigerant capacity can be enhanced in multiphase systems developed by ball milling. The presence of an amorphous phase with  $T_C^{\text{Am}}=244$  K and an intermetallic phase with  $T_C^{\text{Int}}=365$  K is the microstructure responsible for a non-monotonic dependence of RC with fraction of phases. This leads to the clear enhancement of RC observed in this work for samples with the highest amount of the intermetallic compound over the expected behaviour of completely amorphous samples.

After XRD, magnetization and Mössbauer results, a plausible identification of this intermetallic is a Zr-rich supersaturated solid solution fcc  $\text{Fe}_2\text{Zr}$  phase.

## 6. Acknowledgements

This work was supported by the Spanish Ministry of Science and Innovation and EU FEDER (Project MAT 2010-20537), the PAI of the Regional Government of

Andalucía (Project P10-FQM-6462), and the United States Office of Naval Research (Project N00014-11-1-0311).

## 7. References

- 
- [1] K.A. Gschneidner, Jr. and V.K. Pecharsky, *Annu. Rev. Mater. Sci.* 30 (2000) 387.
- [2] M.E. Wood and W.H. Potter, *Cryogenics* 25 (1985) 667.
- [3] R. Caballero-Flores, V. Franco, A. Conde, K. E. Knipling, M. A. Willard, *Appl. Phys. Lett.* 98 (2011) 102505.
- [4] S.C. Paticopoulos, R. Caballero-Flores, V. Franco, J. S. Blázquez, A. Conde, K. E. Knipling, M. A. Willard, to be published.
- [5] J.J. Ipus, H. Ucar, M.E. McHenry, *IEEE Trans. Mag.* 47 (2011) 2494.
- [6] J.J. Ipus, M.E. McHenry, “Influence of Ni and Mn additions on Magnetocaloric Response in  $\gamma$ -(Fe<sub>70-x</sub>Ni<sub>30+x</sub>)<sub>89-y</sub>MnyZr<sub>7</sub>B<sub>4</sub>” contribution to 56<sup>th</sup> Annual Conference on Magnetism and Magnetic Materials
- [7] N.J. Jones, H. Ucar, J.J. Ipus, M.E. McHenry, D.E. Laughlin, *J. Appl. Phys.* 111 (2012) 07A334.
- [8] M.E. McHenry, M.A. Willard, D.E. Laughlin, *Progress in Mater. Sci.* 44 (1999) 291.
- [9] V. Franco, J.S. Blázquez, C.F. Conde, and A. Conde, *Appl. Phys. Lett.* 88 (2006) 42505.
- [10] I. Skorvanek, J. Kovac, J. Marcin, P. Svec, D. Janickovic, *Mater. Sci. Eng. A* 449-451 (2007) 460-463.
- [11] J. Ipus, J. S. Blázquez, V. Franco, A. Conde, *J. Appl. Phys.* 105 (2009) 123922.
- [12] J. Ipus, J. S. Blázquez, V. Franco, A. Conde, *J. Alloys Compd.* 496 (2010) 7-12.

- [13] J. S. Blázquez, J. J. Ipus, C. F. Conde, A. Conde, J. Alloys Compd. (2011), doi:10.1016/j.jallcom.2011.11.084.
- [14] J. J. Ipus, J. S. Blázquez, V. Franco, M. Millán, A. Conde, D. Oleszak, T. Kulik, Intermetallics 16 (2008) 470-478.
- [15] C. Suryanarayana, Prog. Mater. Sci. 46 (2001) 1.
- [16] R. A. Brand, J. Lauer, D. M. Herlach, J. Phys. F: Met. Phys. 12 (1983) 675.
- [17] Y.V.B. de Santanna, M.A.C. de Melo, I.A. Santos, A.A. Coelho, S. Gama, L.F. Cótica, Solid State Commun. 148 (2008) 289–292.
- [18] D.M. Rajkumar, M. Manivel Raja, R. Gopalan, V. Chandrasekaran, J. Magn. Mater. 320 (2008) 1479–1484.
- [19] L. F. Kiss, G. Huhn, T. Kemény, J. Balogh, D. Kaptás, J. Magn. Mater. 160 (1996) 229-232.
- [20] N. Mattern, W. X. Zhang, S. Roth, H. Reuther, C. Baetz, M. Richter, J. Phys.: Condens. Matter 19 (2007) 376202.
- [21] T. Kemény, D. Kaptás, J. Balogh, L. F. Kiss, T. Pusztai, I. Vincze, J. Phys.: Condens. Matter 11 (1999) 2841-2847.
- [22] M. Migliorini, J. M. Greneche, B. Idzikowski, Mater. Sci. Eng. A304-306 (2001) 937-940.
- [23] P. Gülich, E. Bill, A. X. Trautwein, Mössbauer Spectroscopy and Transition Metal Chemistry. Fundamentals and Applications, Springer-Verlag, Berlin, 2011.

### Figure captions

Figure 1. XRD patterns of as-milled samples and samples heated up to above its crystallization temperature.

Figure 2. Magnetic entropy change as a function of temperature for the different studied samples at a maximum applied field of 1.5 T.

Figure 3. RC values at a maximum applied field of 1.5 T of the different studied samples using three different definitions (see text for details). Lines are a guide to the eye.

Figure 4. Magnetization at 0.05 T (solid circles) and average hyperfine field (hollow circles) as a function of temperature of measurement for the sample milled at 286 rpm after the second milling step. Triangles indicate the Curie temperature of the amorphous,  $T_C(1)$ , and the intermetallic phase,  $T_C(2)$ . The inset shows the thermal derivative of magnetization curve.

Figure 5. Mössbauer spectra of three as-milled samples at three different temperatures. Hollow circles correspond to experimental data and line corresponds to fit curve.

Figure 6. Average isomer shift and fraction of HFD contribution above 5 T as a function of the temperature of measurement.

Figure 7. Refrigerant capacity as a function of fraction of HFD contributions above 5 T. Dashed line is a guide to the eye inspired in the theoretical results from Ref. [3].

Figure 8. Technical saturation magnetization as a function of average hyperfine magnetic field. Lines are linear fitting to the corresponding experimental data.

Figure 1 (web version)

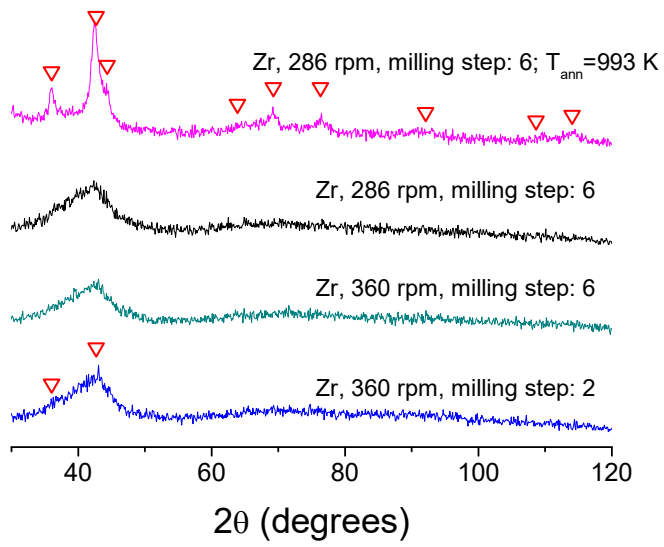


Figure 2 (web version)

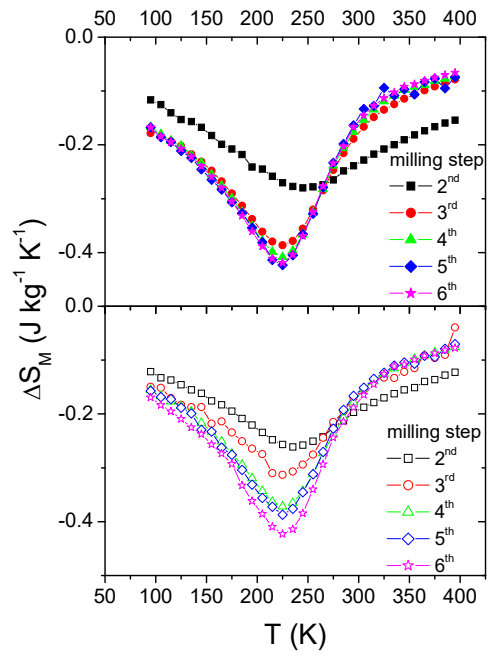


Figure 3 (web version)

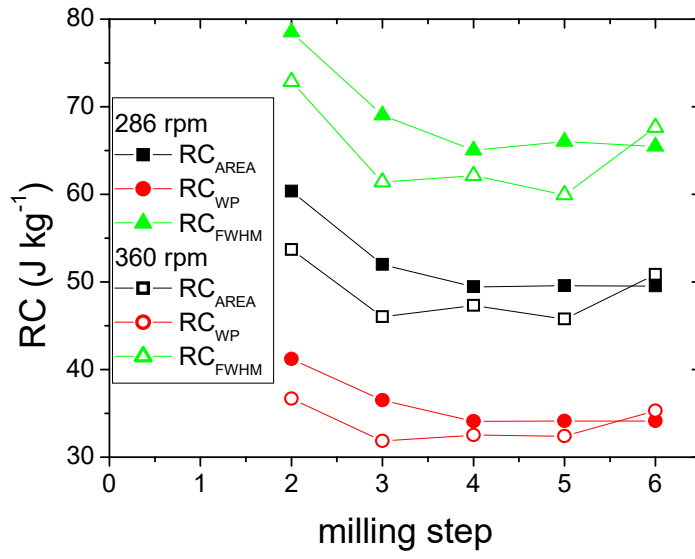




Figure 4 (web version)

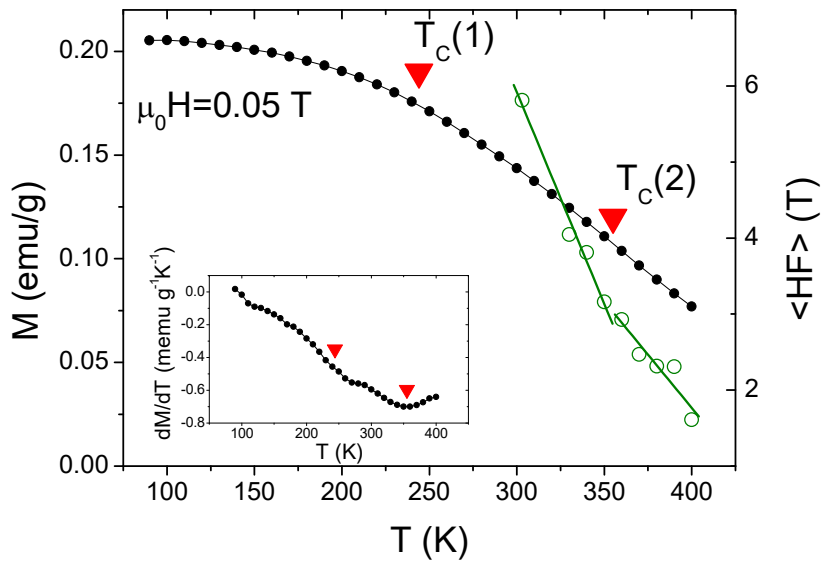


Figure 5 (web version)

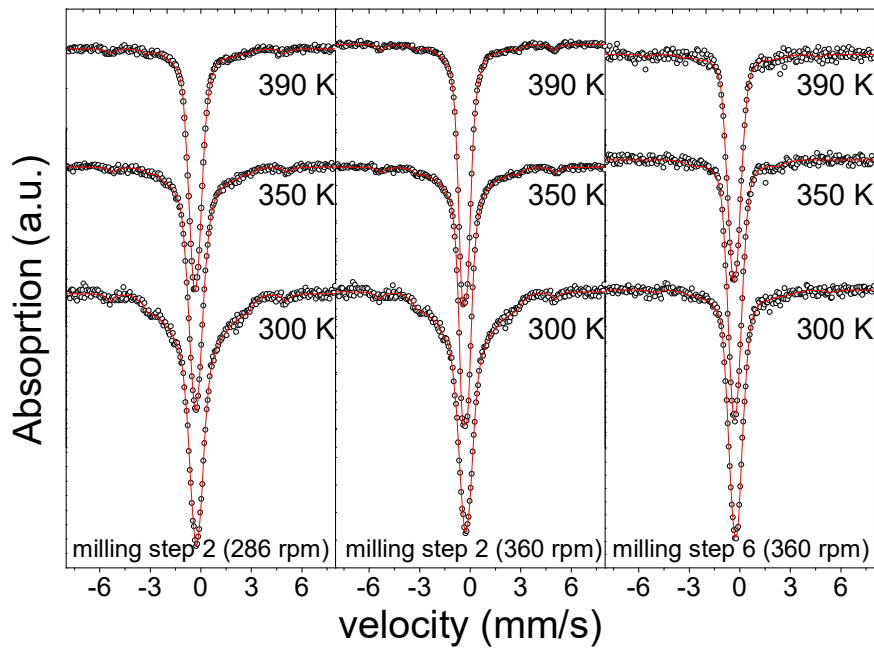


Figure 6 (web version)

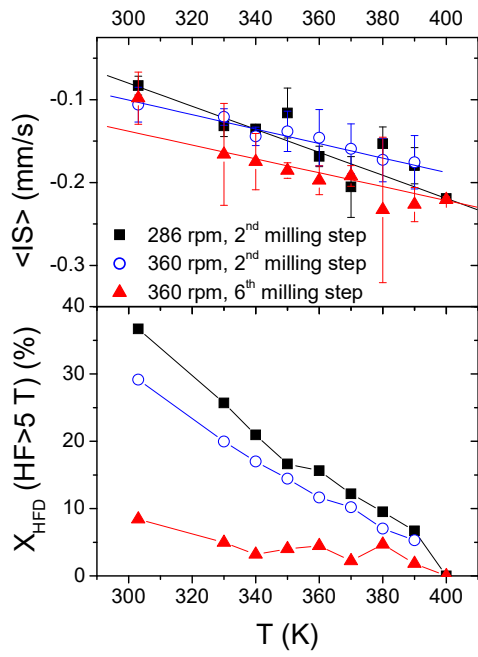


Figure 7

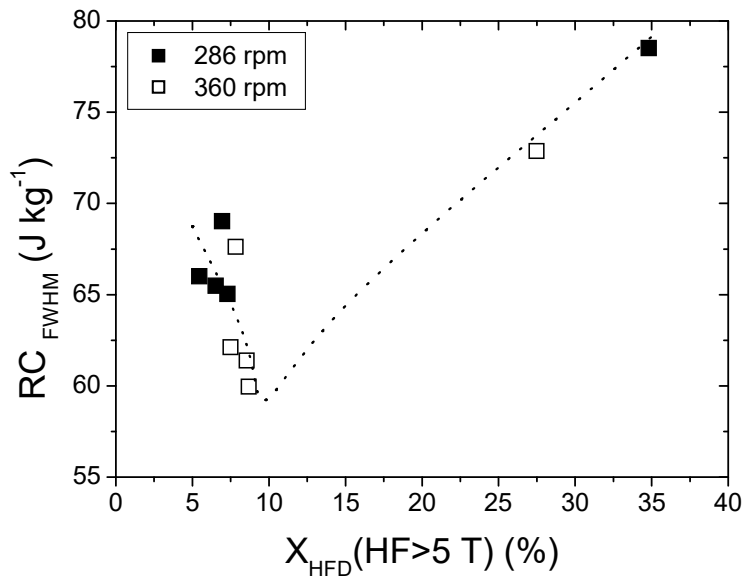


Figure 8 (web version)

